ELSEVIER

Journal of Power Sources 107 (2002) 167–172

JOURNAL OF POWER SOURCES

www.elsevier.com/locate/jpowsour

In situ EC-AFM study of effect of lignin on performance of negative electrodes in lead−acid batteries

I. Ban[a,*], Y. Yamaguchi[a], Y. Nakayama[a], N. Hirai[b], S. Hara[b]

[a]*Yuasa Corporation, 2-3-21 Kosobe-cho, Takatsuki, Osaka 569-1115, Japan*

[b]*Department of Materials Science and Processing, Graduate School of Engineering, Osaka University, 2-1 Yamadaoka, Suita, Osaka 565-0871, Japan*

Received 1 August 2001; accepted 30 October 2001

Abstract

The effect of lignin, which is an important additive for the negative electrode in lead–acid batteries, is studied on lead electrodes in sulfuric acid by means of potentiostatic transient measurements and in situ electrochemical atomic force microscope (EC-AFM) observations. During oxidation of the electrodes, it is confirmed that the current transition in electrolyte with 20 ppm lignin gives a broad, hill-like curve, while that in electrolyte without lignin is a sharp peak. Nevertheless, there is little difference in electrode capacity in each electrolyte throughout the whole oxidation. In electrolyte with lignin, in situ EC-AFM examination reveals a uniform deposition of lead sulfate crystals after oxidation of the electrode. These results suggest that lignin adsorbs on the electrode surface and promotes uniform diffusion of lead ions near the surface during oxidation.

Keywords: Electrochemical atomic force microscopy; Expander; In situ observation; Lead–acid battery; Lignin; Negative electrodes

1. Introduction

Lead–acid batteries are widely used in automotive and standby applications [1]. In order to conserve energy and alleviate environmental problems, research is being undertaken in the development of novel lead–acid batteries for electric vehicles (EVs), electric hybrid vehicles (HEVs), load-leveling (LL) installations, etc. [1–5]. Since these new applications demand a higher performance from the battery, a detailed understanding of the electrode reaction is very important.

This work reports the application of an electrochemical atomic force microscope (EC-AFM) for in situ observation of the electrode reactions in sulfuric acid electrolyte [6–9]. The reactions of the lead–acid battery have traditionally been studied by means of the current and the potential obtained by using conventional electrochemical techniques which include discharge−charge tests. In many cases, the morphology changes which occur on the electrode surface during reaction have been only surmised from ex situ scanning electron microscopy (SEM) analysis. The novel EC-AFM technique overcomes the shortcomings of conventional methods, and it has made possible the direct observation of the reaction process of the lead electrode in the electrolyte during oxidation and reduction [6–8]. Moreover, we have succeeded in the direct observation of the morphology changes on the lead dioxide electrode surface, though this is considered to be more difficult than that for the lead surface [9].

The study of additives for the negative electrode in the lead−acid battery has recently gained in importance in order to improve battery life, charge-acceptance, etc. Lignin (so-called 'organic expander') is of particular interest as it affects not only the cold-cranking ability (CCA) and cycle life, but also exerts a beneficial effect on the overall performance of the negative electrode. According to Francia et al. [10], lignin adsorbs on the electrode surface and influences the electrochemical behavior of the electrode. Pavlov et al. [11] examined the chemical composition of lignin. They proposed that the most effective lignin for starting–lighting–ignition (SLI) battery performance should have a low average molecular weight, a high –COOH content, low contents of $–OCH_3$ and organic S, optimum Ar–OH content, and high purity. It was also concluded that lignins with different chemical compositions should be selected for different types of battery application.

If the mechanism of the effect of lignin on the negative electrode can be understood precisely, it may be possible to

* Corresponding author. Tel.: +81-726-85-2681; fax: +81-726-85-3070.
E-mail address: ikumi_ban@yuasa-jpn.co.jp (I. Ban).

0378-7753/02/$ – see front matter
PII: S0378-7753(01)01002-3

synthesize a new organic expander that is more suitable for the electrode reaction. This study using the in situ EC-AFM technique is seen as the first step to clarifying the behavior of lignin. To this end, the changes of electrode morphology on oxidation in electrolyte either with or without lignin are observed by EC-AFM and compared.

2. Experimental

2.1. Equipment

The EC-AFM equipment is shown schematically in Fig. 1. The system is composed of a control unit (NanoScope IIIa) made by Digital Instruments Co., a microscope (Pico SPM) made by Molecular Imaging Co., an electrochemical cell, and some electrochemical devices. EC-AFM studies were performed with a commercial Si_3N_4 cantilever with integral gold-coated tips. The electrochemical cell comprised a lead electrode as the working electrode, a PbO_2 electrode as the counter electrode, and a Hg/Hg_2SO_4 electrode in 50 mM H_2SO_4 solution as the reference electrode. All potentials reported here are referred to this electrode. The electrochemical operations were carried out by using a potentio/galvanostat (model HA501G) with a function generator (model HB105) made by Hokuto Denko Co. The current change was measured with a digital scope (model DL716) made by Yokogawa Electric Co. and the measuring interval was 20 ms.

2.2. Preparation of EC-AFM cells without lignin

An electrode was prepared from pure-lead sheet (99.99%). Sulfuric acid solution with a concentration of 1.250 g cm^{-3} (approximately 34 wt.%) was used. Oxygen dissolved in the electrolyte was removed by bubbling argon gas for 3 h beforehand.

The electrode surface was chemically etched with acetic acid to remove the existing lead oxide layer, and then washed with ethanol. The electrode was placed in a cell as the working electrode and had an exposed area of about 1.25 cm^2. The cell was then filled with electrolyte. A potential of −1400 mV was applied for 30 min to the electrode to reduce completely the surface. This was followed by further reduction at −1200 mV for 30 min. After this reduction, no lead sulfate crystals were found on the surface by EC-AFM observation at the rest potential of −1085 mV.

In order to provide the electrode with an electrochemically-active surface, it was subjected to five cyclic voltammetric (CV) cycles between −1400 and −800 mV at a sweep rate of 20 mV s^{-1}. The electrode was then reduced again by holding at a potential of −1400 mV for 30 min, followed by −1200 mV for 30 min. No lead sulfate crystals were observed on the electrode surface by EC-AFM observation at the rest potential of −1090 mV. Next, an EC-AFM observation of the electrode in electrolyte without lignin was made by using this prepared cell. All tests were performed at a temperature of 25 °C. An outline of the cell preparation processes is given in Fig. 2.

2.3. Preparation of EC-AFM cells with lignin

In case of cell preparation with lignin, the procedure given in Section 2.2 was repeated. The rest potentials of this electrode after the first and the second reduction were −1085 and −1090 mV, respectively. The following procedure was then adopted to examine the effect of lignin.

The electrolyte of the cell was replaced with 1.250 g cm^{-3} acid containing 20 ppm lignin. The lignin used was 'Vanillex N' made by Nippon Paper Industries Co. Oxygen dissolved

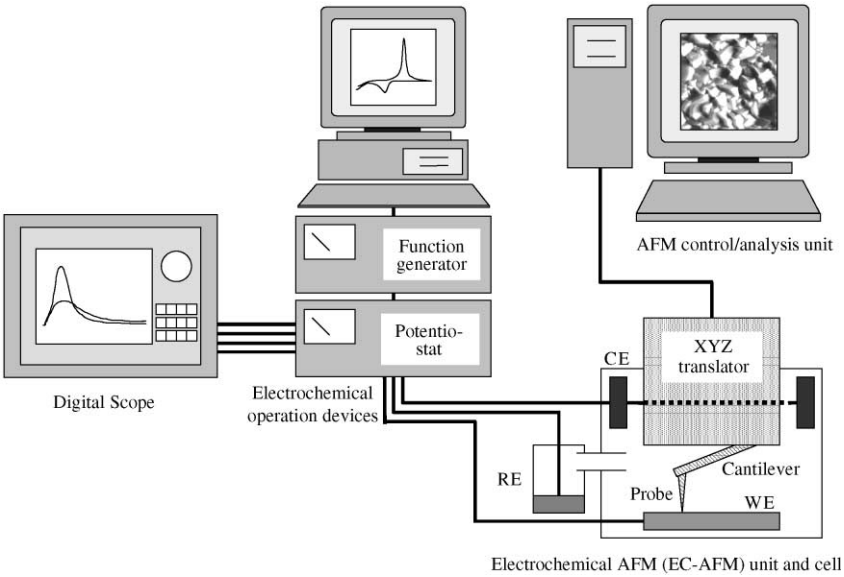

Fig. 1. Schematic of EC-AFM equipment. WE is pure-lead electrode, CE is PbO_2 counter electrode, and RE is Hg/Hg_2SO_4 reference electrode.

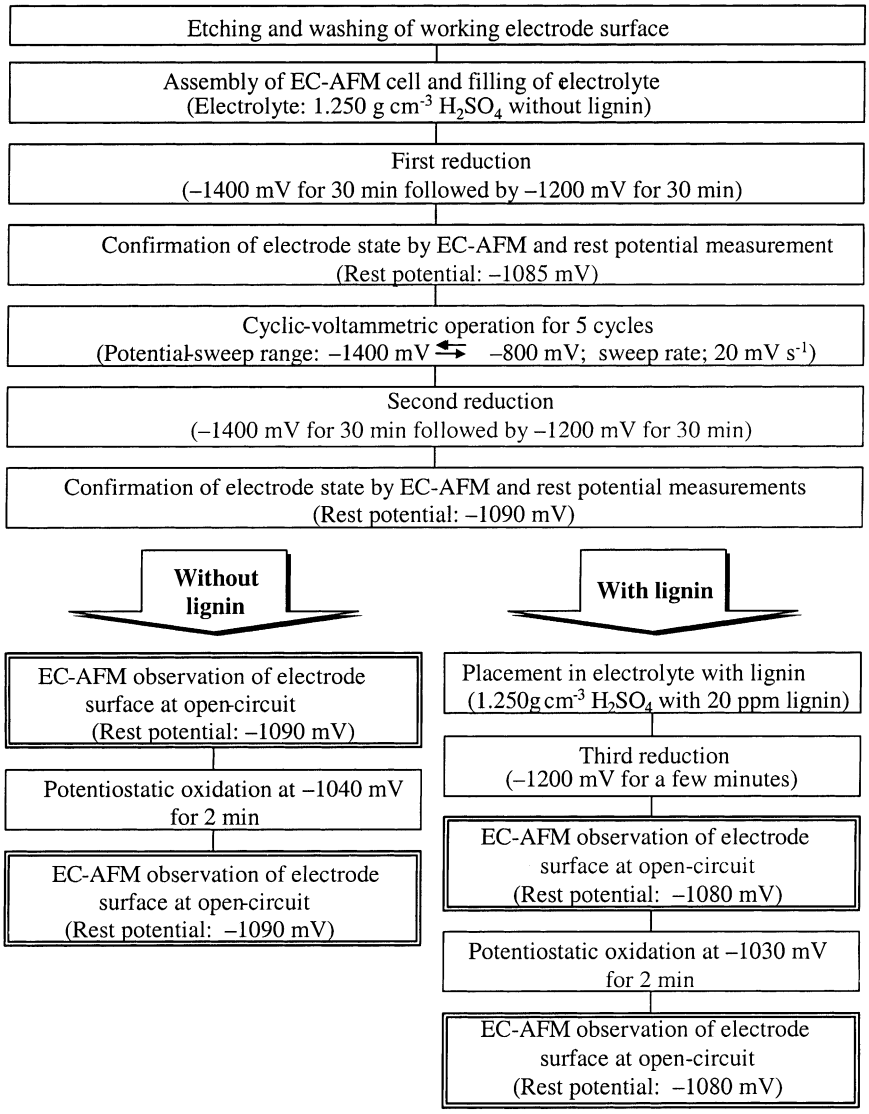

Fig. 2. Experimental procedure for cell preparation and EC-AFM observations. All potentials are referred to an Hg/Hg_2SO_4 electrode in 50 mM H_2SO_4 solution. Experiments performed at 25 °C.

in the electrolyte was removed by bubbling argon gas for 3 h beforehand. The electrode was reduced for a few minutes at a potential of −1200 mV. All tests were performed at a temperature of 25 °C. An outline of these cell preparation processes is also shown in Fig. 2.

2.4. EC-AFM observation with oxidation of the electrodes

Four in situ EC-AFM observations were carried out before and after oxidation of each electrode. The AFM image area and the observation time were set at 10 μm × 10 μm and 52 s, respectively.

The electrode surface in electrolyte without lignin was observed by EC-AFM at the open-circuit state (rest potential: −1090 mV) before oxidation. The electrode was then oxidized at −1040 mV, i.e. at 50 mV higher than its rest potential, for 2 min. The current transient and potentials were recorded at intervals of 20 ms throughout the course of the oxidation. An EC-AFM study was again made at open-circuit to observe the change in morphology of the electrode surface.

A similar experimental sequence was applied to a cell filled with electrolyte that contained lignin. Since the rest potential the working electrode was −1080 mV, the potentiostatic oxidation was performed at a potential of −1030 mV. This procedure is also shown in Fig. 2.

All tests were conducted at a temperature of 25 °C and carried out in an argon gas chamber to avoid oxidation of the electrode.

3. Results

The current responses of two electrodes in electrolyte without lignin are shown in Fig. 3a; the cyclic applied potential for oxidation and reduction is given in Fig. 3b. The solid and broken lines are for the different runs of

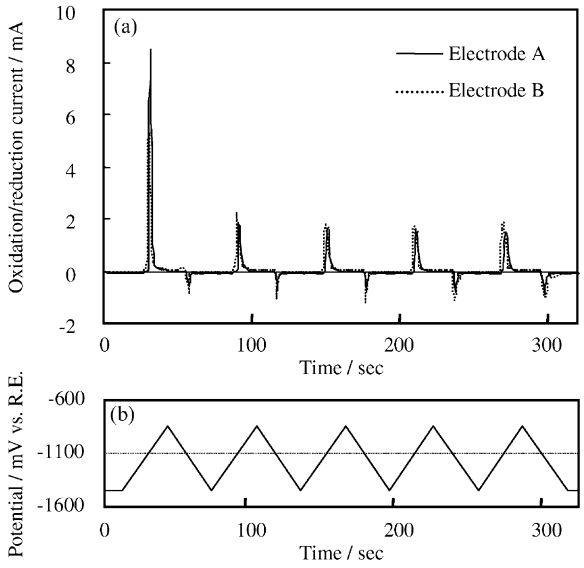

Fig. 3. Changes in both oxidation/reduction current (a) and potential (b) of two lead electrodes in the 1.250 g cm^{-3} sulfuric acid electrolyte without lignin during five cycles of CV.

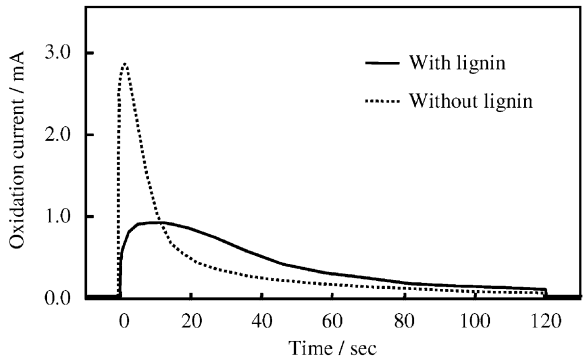

Fig. 4. Current transients of electrodes in electrolyte with and without lignin during potentiostatic oxidation at −1030 mV vs. RE (with lignin) and −1040 mV vs. RE (without lignin).

electrodes 'A' and 'B'. Similar current transients are observed for these two electrodes, and this confirms that the difference in their properties was negligible. The oxidation peaks of each electrode become smaller with cycling. This behavior may be due to insufficient reduction at the applied fast sweep rate of 20 mV s^{-1}. The electrodes were then reduced again for 1 h and EC-AFM observations confirmed that no lead sulfate crystals remained on either electrode after the reduction. Electrode 'A' was subjected to further reduction at −1200 mV for a few minutes after substitution of the electrolyte with one that contained lignin.

The oxidation current transients of the electrodes with and without lignin are presented in Fig. 4. These were measured during potentiostatic oxidation at a potential which was 50 mV higher than the respective rest potential. The transient in the presence of 20 ppm lignin is a broad, 'hill-like' curve, whereas that in the absence of lignin is a sharp peak. The electrical capacity of each electrode, which was integrated from the data, was 43.11 mA s (no lignin) and 44.25 mA s (with lignin). Clearly, the addition of lignin has little effect on the capacity.

EC-AFM images of each electrode surface before/after potentiostatic oxidation are displayed in Fig. 5. The

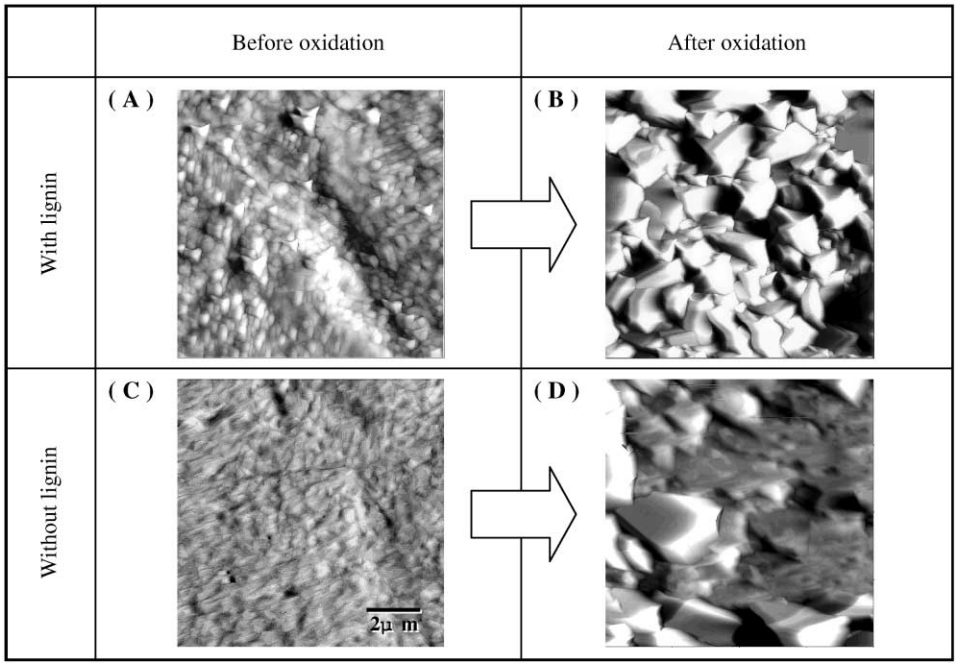

Fig. 5. EC-AFM images of electrode surfaces observed before/after potentiostatic oxidation. (A) Image before oxidation with lignin; (B) image after oxidation with lignin; (C) image before oxidation without lignin; (D) image after oxidation without lignin.

morphologies of the surfaces in the electrolyte with lignin before and after oxidation are labelled as (A) and (B), respectively and those in the electrolyte without lignin before and after oxidation are marked as (C) and (D), respectively. Before oxidation, the surface with lignin (A) appears to be uneven with many small granular materials, and is somewhat similar to that without lignin (C). Lead sulfate crystals were deposited on each surface during the oxidation process, whether the electrolyte contained lignin or not. There is, however, a difference in the form of the crystals. In the electrolyte with lignin, the deposition of lead sulfate crystals is uniform over the surface after oxidation. Without lignin, however, the lead sulfate crystals are dispersed irregularly.

Based on these results, a model for the effect of lignin on the lead electrode has been developed and is described in Section 4.

4. Discussion

The oxidation current transients with and without lignin shown in Fig. 4 agree well with the results obtained by Francia et al. [10]. Thus, it is confirmed that the present measurement is a very useful technique for examining the effect of lignin. Based on the difference in the transients, Francia et al. [10] considered that the expander adsorbs on the electrode surface and influences the dissolution–precipitation mechanism which occurs during the oxidation reaction. Our results from in situ EC-AFM observations performed during a similar electrochemical experiment support this view.

In addition, we have developed an understanding of the mechanism of the lignin that is based on both an adsorbed form of the lignin on the electrode surface and its influence on the diffusion of lead ions during the oxidation reaction. The model is shown schematically in Fig. 6.

Generally, lead ions start to saturate the electrolyte immediately after the oxidation potential is applied. The deposition of lead sulfate crystals on the electrode then occurs due to the super-saturated state of the ions [7]. In our studies, it is considered that deposition of the crystals begins at 1.6 s in the absence of lignin (Fig. 4). This process has been called the ‘dissolution–precipitation reaction’ [12].

The dissolution of lead ions in the electrolyte without lignin during oxidation is shown in Fig. 6a–c. If a thin, discontinuous layer of lead oxide or an impurity exists on the electrode surface, then the dissolution–precipitation reaction of the ions will occur only at sites not covered with such a layer, as shown in the drawings. We suggest that this process accounts for the sparse deposition of lead sulfate crystals shown in image (D) of Fig. 5.

A model of the lignin effect is illustrated in Fig. 6d–g. The drawing (d) represents the initial effect of lignin. When absorbed on the electrode, the lignin acts to remove the obstructive layer from the electrode surface by a reductive or

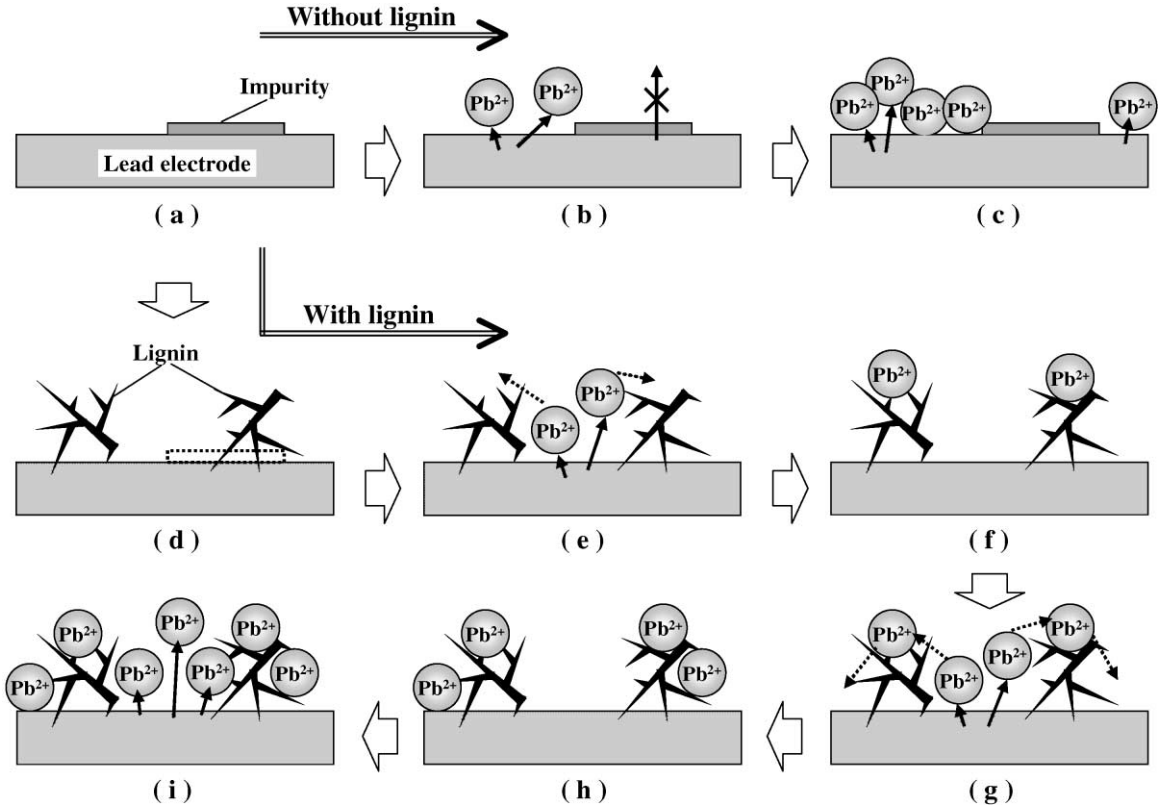

Fig. 6. (a–i) Model of lignin effect on lead electrode during oxidation.

solvent effect. In other words, we conclude that the lignin functions as a 'cleaning' process for the electrode surface, like a surfactant.

Drawing (e) shows the initial dissolution of lead ions when the oxidation potential is applied. The lead ions are dissolved from sites where lignin is not adsorbed. We further suggest that the lead ions to diffuse from their dissolution sites to further locations on the lignin molecules. This transfer of the lead ions is the second effect of the adsorbed lignin, and is illustrated schematically in Fig. 6e–g. When such a phenomenon occurs on the electrode, the concentration of lead ions at the dissolution site is maintained at a comparatively low value. Therefore, the dissolution of the lead ion continues until the concentration rises sufficiently for lead sulfate deposition to take place over the whole of the electrode surface.

We conclude that both the broad, hill-like transition of the oxidation current and the uniform deposition of lead sulfate crystals are caused by the lignin effect. Moreover, the electrical capacity in the two electrolytes is similar. This fact strongly supports the validity of our model.

It should be noted that the above-mentioned effects of lignin are useful only when the quantity of the additives is suitable for the electrode area. If too much lignin is added, it suppresses dissolution of the lead ions because the lignin adsorption area becomes too wide or its adsorption layer becomes too thick. Indeed, it is found that the performance of lead–acid batteries declines when too much lignin is added to the negative electrode. Therefore, the quantity of lignin should be selected carefully when designing negative electrodes of lead–acid batteries.

5. Conclusions

The following results have been obtained for behavior of lignin additives in the negative electrode of the lead–acid batteries.

1. The oxidation current transition of an electrode in electrolyte with 20 ppm lignin is in the form of a broad, hill-like curve, but becomes a sharp peak in the absence of lignin. There is little difference in the electrical capacity, whether the electrolyte contains lignin or not.
2. In electrolyte with lignin, a uniform deposition of lead sulfate occurs on the electrode surface after oxidation.
3. Based on the above results, a model for the lignin effect is proposed. This assumes that the lignin adsorbed on the electrode encourages a uniform diffusion of lead ions during the oxidation reaction.

It is confirmed that in situ EC-AFM observation is a useful technique for gaining an understanding of the lignin effect. Also, we expect that the mechanisms of other types of expander can be clarified in detail by this new method.

References

[1] K. Hirakawa, S. Takahashi, M. Morimitsu, Y. Yamaguchi, Y. Nakayama, Yuasa-Jiho 87 (1999) 42–46.
[2] S. Takahashi, K. Hirakawa, H. Moeimitsu, Y. Yamaguchi, Y. Nakayama, Yuasa-Jiho 88 (2000) 34–38.
[3] T. Kameda, E. Hojo, S. Nagai, Y. Nakayama, K. Imai, H. Takagi, Yuasa-Jiho 86 (1999) 36–40.
[4] E. Hojo, Y. Nakayama, T. Koike, Yuasa-Jiho 87 (1999) 11–16.
[5] M. Hosokawa, N. Yamada, K. Hasegawa, Y. Nakayama, M. Yokoh, K. Ariga, T. Takeda, in: Proceedings of the 16th International Electric Vehicle Symposium (EVS-16), CD-ROM, 1999.
[6] Y. Yamaguchi, M. Shiota, Y. Nakayama, N. Hirai, S. Hara, J. Power Sources 85 (2000) 22–28.
[7] Y. Yamaguchi, M. Shiota, Y. Nakayama, N. Hirai, S. Hara, J. Power Sources 93 (2001) 104–111.
[8] Y. Yamaguchi, M. Shiota, Y. Nakayama, N. Hirai, S. Hara, J. Power Sources 102 (2001) 155–161.
[9] M. Shiota, Y. Yamaguchi, Y. Nakayama, K. Adachi, S. Taniguchi, N. Hirai, S. Hara, J. Power Sources 95 (2001) 203–208.
[10] C. Francia, M. Maja, P. Spineli, F. Saez, B. Martinez, D. Marin, J. Power Sources 85 (2000) 102–109.
[11] D. Pavlov, B.O. Myrvold, T. Rogachev, M. Matrakava, J. Power Sources 85 (2000) 79–91.
[12] J.L. Weininger, J. Electrochem. Soc. 121 (1974) 1454–1457.